



# Short communication: New analytical approach on (U-Th)/He dating of Fe-hydroxide with an example using goethite from the Amerasian Basin, Arctic Ocean

5 Olga Valentinovna Yakubovich<sup>1,2</sup>, Natalia Pavlovna Konstantinova<sup>2,3</sup>, Maria Olegovna Anosova<sup>4</sup>, Mary Markovna Podolskaya<sup>5</sup>, Elena Valerevna Adamskaya<sup>2</sup>

<sup>1</sup>Department of geochemistry, Saint-Petersburg University, St. Petersburg, 199034, Russia

<sup>2</sup>Laboratory of Isotope Geology, Institute of Precambrian Geology and Geochronology RAS, St. Petersburg, 199034, Russia

<sup>3</sup>Institute for Geology and Mineral Resources of the Ocean (VNIIOkeangeologia), St. Petersburg, 190121, Russia

<sup>4</sup>Vernadskiy institute of Geochemistry and Analytical Chemistry, Moscow, 119991, Russia

10 <sup>5</sup>AnalyteMe, Reus, Tarragona, 43201, Spain

*Correspondence to:* Olga Yakubovich (olya.v.yakubovich@gmail.com)

## Abstract

We propose a new analytical approach for (U-Th)/He dating of Fe-hydroxides, that includes sealing samples in quartz ampoules and demonstrates its suitability as a reliable tool for the investigation of geological processes. The (U-Th)/He ages of goethite clasts and vein from Fe- and Mn-oxide mineralization rocks recovered from the slope of Chukchi Borderland in the Amerasia Basin demonstrate remarkable reproducibility, yielding a weighted mean age of  $8.6 \pm 0.3$  Ma (n=4) and  $4.8 \pm 0.4$  Ma (n=2), respectively, providing insights into the Neogene mineralization history of the region. This study also focuses on the sample preparation technique, that might influence the (U-Th)/He ages. Our data indicate that significant fraction of U can be leached from the goethite during sonication by distilled water which might result in over-dispersed (U-Th)/He ages.

## 1. Introduction

The (U-Th)/He dating method is based on the alpha-decay of U and Th that produce helium atoms. The accumulated <sup>4</sup>He component is used to determine the mineral age. Traditionally, the <sup>4</sup>He isotopic systems have been successfully applied to low-temperature thermochronology (Farley and Stockli, 2002). Recent developments in understanding how helium behaves in various minerals have extended the method applicability in geochronological studies (Yakubovich et al. 2019; Shukolyukov et al. 2012; Flowers et al. 2023 and references therein).



Fe-oxides and Fe-hydroxides, including goethite ( $\alpha$ -FeO(OH)), lepidocrocite ( $\gamma$ -FeO(OH)), hematite ( $\alpha$ -Fe<sub>2</sub>O<sub>3</sub>), maghemite ( $\gamma$ -Fe<sub>2</sub>O<sub>3</sub>) and magnetite ( $\text{Fe}^{2+}\text{Fe}^{3+}_2\text{O}_4$ ), typically contain trace amounts of U and Th and therefore have been recognized as a potential geochronometer tool from the early days of geochronology (Strutt, 1908, 1909).

30 Goethite is one of the most common Fe- (oxy)hydroxide mineral which is formed during hydrolyzation of the rocks, implying it to be a desired mineral for dating various surface and subsurface geological processes. Helium diffusion studies revealed sufficient <sup>4</sup>He retentivity in goethite an the range of the near-surface temperatures and make the mineral suitable for the (U-Th)/He weathering geochronology (Shuster et al., 2005).

The (U-Th)/He dating of goethite was applied successful in dating of weathering profiles (Monteiro et al., 2014; Riffel et al., 35 2016; Ansart et al., 2022), supergene ore formation (Vasconcelos et al., 2013; Heller et al., 2022; Verhaert et al., 2022), and diagenetic transformations (Reiners, 2014). The approach was also implemented successful in dating deep-sea hydrothermal Fe-oxide mineralization (Benites et al., 2022). However, the dating of hydrogenetic Fe-Mn crusts is not robust due to the significant content of extraterrestrial He-rich dust and their high porosity, that prevent the accumulation of radiogenic He (Basu et al., 2006).

40 The (U-Th)/He dating of surface processes is challenging due to the multistage Fe-hydroxides formation. Several generations of the same phase intimately intergrow in a millions years time span (Vasconcelos et al., 2013; Monteiro et al., 2014; Heller et al., 2022). Presence of small inclusions of U- and Th-bearing contaminants may add difficulties to the interpretation of the isotopic results. Thus, high-resolution mineralogical and paragenetic characterization of the sample is required which typically includes optical observations accompanied by XRD, SEM and chemical analyses (EPMA).

45 From the analytical point of view (U-Th)/He dating of goethite is challenging as well. The distribution of U and Th in the mineral is inhomogeneous (Shuster and Farley, 2005), therefore parental and daughter isotopes should be measured in the same sample. Helium release from the goethite must be carried out under strictly controlled laboratory heating conditions; otherwise, U and Th may be lost from the grains during He extraction rendering the results inaccurate (Vasconcelos et al., 2013). There are several approaches to overcome this issue such as heating in the presence of oxygen (Hofmann et al., 2020), 50 using double-aliquot (Wernicke and Lippolt, 1993; Pidgeon et al., 2004), or multi-aliquot procedures (Wu et al., 2019). The last two require remarkably larger amount of material.

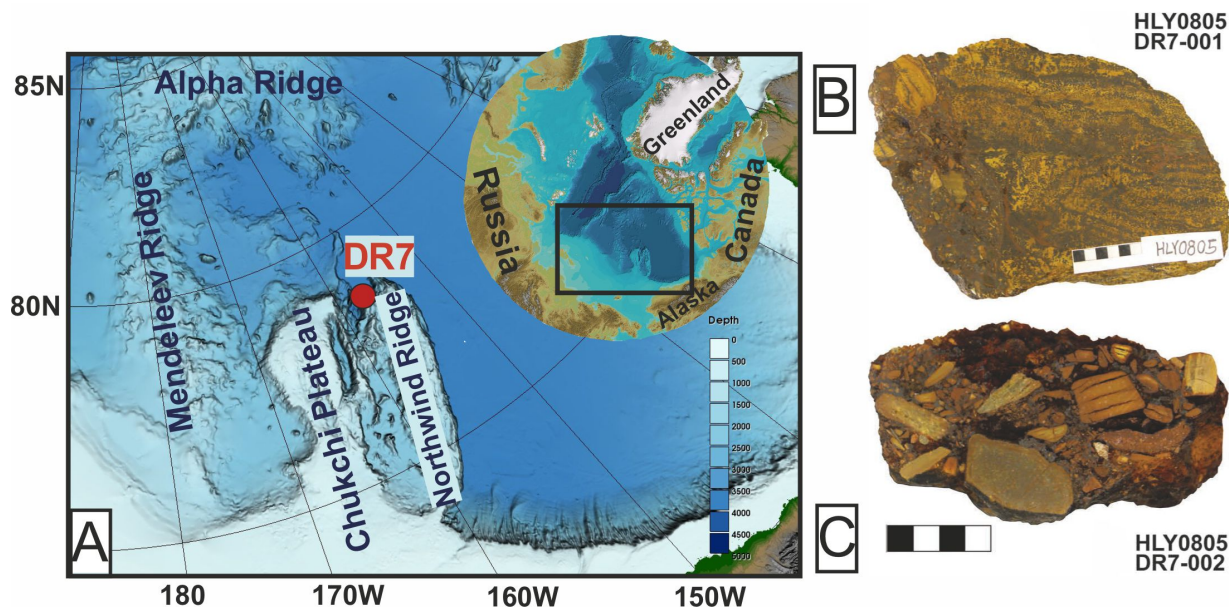
Here, we propose the alternative (U-Th)/He dating methodology using an example of goethite from the Chukchi Borderland, Arctic Ocean. The technique was originally developed for (U-Th)/He dating of native gold (Yakubovich et al. 2014) and pyrite (Yakubovich et al. 2020).



## 55 2. Samples

The Amerasia basin of the Arctic Ocean remains one of the Earth's least explored region (Brumley et al., 2015). The Chukchi Borderland and Mendeleev Ridge are known as Paleozoic continental blocks that occur within the Amerasia Arctic Ocean. During the U.S. and Russian research cruises fragments of Fe- and Mn-oxide mineralization were collected from several sites of the northern Chukchi Borderland and central Mendeleev Ridge (Fig. 1A; Hein et al., 2017; Konstantinova et al., 2017). The subject of this study is the age dating of samples from dredge haul DR7 collected from 3400 m water depth (coordinates 60 78.53N, 156.68W).

The DR7 dredge haul consists of rock fragments that are extensively altered and finely sheared. Two different rock types were found. First one shows alternating yellow-brown and dark-brown layers, with dendrites of the dark-brown material in the yellow-brown laminae (Fig. 1B). Both layer types mainly comprise Fe-(hydro)oxides, but the dark-brown layers have a higher Mn-oxide content. Another rock type in DR7 is a breccia with poorly sorted predominantly angular to subangular clasts (Fig. 65 1C), that include pure Fe oxyhydroxide, basalt, and altered metasedimentary rocks. Mn- or Fe-oxide dendrites are found in some larger clasts. The breccia cement is composed predominately of dark brown Fe-oxyhydroxides with submetallic grey areas. The structure varies from botryoidal to massive to cellular-like. The breccia is predominantly cement-supported, indicating replacement during Fe- and Mn-oxide mineralization.



70

**Figure 1. (A) Regional setting of the Amerasia Basin (inset) and location map of the DR7 dredge haul; (B) cut section images of the main sample types; all subsamples for age dating are from DR7-001.**



The dominant mineral in the mineralized samples based on X-ray diffractions is goethite and possibly lesser amounts of ferroxhyte ( $\delta$ -FeOOH) and ferrihydrite [ $\text{Fe}^{3+}_{4-5}(\text{OH},\text{O})_{12}$ ] (Table 1). The darker colored goethite has better crystallinity than the paler ones. Based on SEM-EDS studies (Fig. 2), Fe-oxides crystallite sizes of cement and replacements vary from submicrometer to a few micrometers, rarely up to 120  $\mu\text{m}$ . Birnessite and 10Å manganates (todorokite, busserite, or asbolane) and  $\delta$ -MnO<sub>2</sub> (vernadite) occur as well. Relict host-rock minerals include quartz, feldspar, mica, and clay minerals. Clinochlore (chlorite) is ubiquitous in the DR7 samples. Among the U-bearing minerals, single grains of zircon and monazite were observed (Fig. 2).

80 **Table 1. XRD Mineralogy of Crystalline Phases of DR7 Sample from the Amerasia Arctic Ocean.**

Sample ID	Description	Major	Moderate	Minor
DR7-001-L1A	Cement from breccia	Goethite	Quartz, Birnessite	TAM
DR7-001-L1B	Glassy Fe-rich clast	Goethite	--	--
DR7-001-L2B	Fe-rich dark-brown lamina	Goethite, Birnessite	Clinochlore, Quartz, Plagioclase	$\delta$ -MnO <sub>2</sub> , TAM
DR7-001-L2D	Reddish vein	Goethite, Quartz	Clinochlore, Plagioclase, Mica	Birnessite, TAM(?)
DR7-001-L2E	Fe-Mn lamina	Birnessite, Goethite	TAM(?), Quartz	Plagioclase

Major >25%, Moderate 5-25%, Minor <5%. TAM is 10Å Manganates = todorokite, busserite, or asbolane. Goethite may also include ferroxhyte or ferrihydrite.

85 Comment: X-ray diffraction mineralogy was completed using a Malvern Panalytical X'Pert Powder X-ray diffractometer (XRD) with CuK $\alpha$  radiation and graphite monochromator run from 4° to 70° 2 $\theta$  with a step size of 0.02° 2 $\theta$  at 40 kV and 45 mA at USGS, PCMSC lab in 2017. Digital scans were analyzed using Philips X'Pert High Score Plus software to analyze X-ray reflections and identify possible mineral phases.

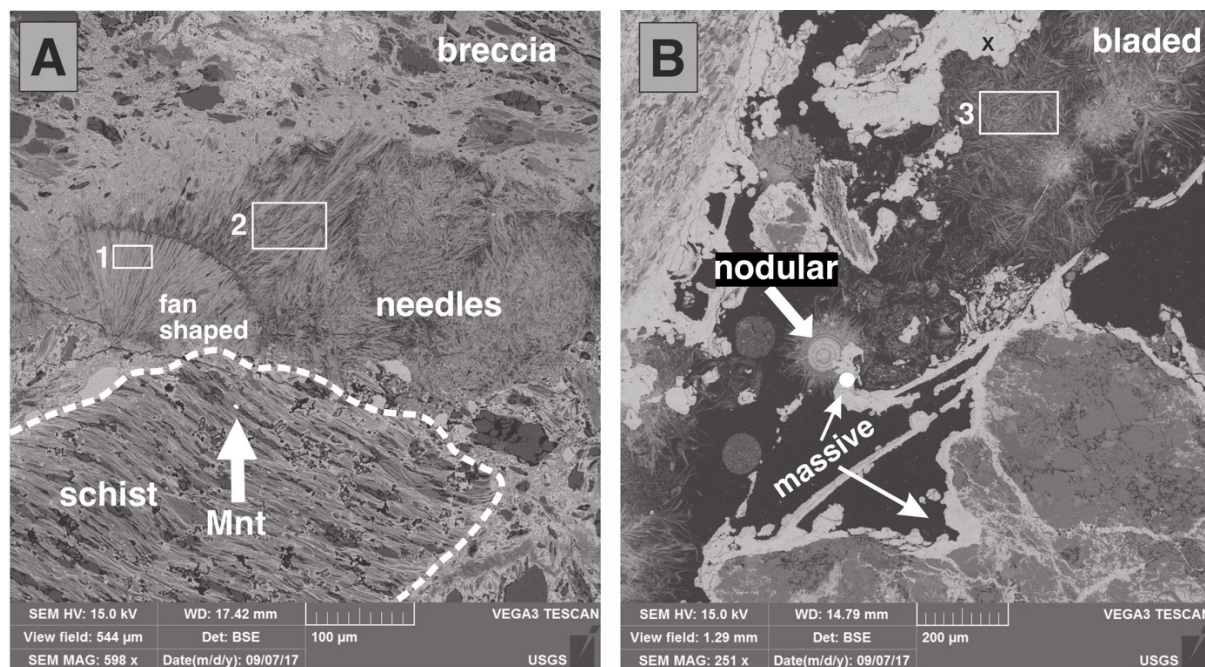


Figure 2. Backscatter SEM photomicrograph images of sample DR7-001 and DR7-002 from polished thin sections; (A) fan-shaped (26% Fe, 17% Mn for box 1), needle (28% Fe, 15% Mn for box 2), and massive cements of Fe and Mn oxides in the breccia part of sample DR-001; note schist grain in the lower left quadrant with a bright monazite grain (Mnt); (B) cement of breccia: bladed (box 3: 29% Fe, 35% Mn), nodular (white arrow: 33% Fe, 25% Mn), and massive (white dot: 68% Fe; black x: 35% Fe, 29% Mn) Fe- and Mn-oxide cements; bladed cement consists of discrete Mn-oxide and Fe-oxyhydroxide blades, and Fe and Mn contents vary for each laminae in the micronodule.

90

Polished thin sections were carbon coated and used for SEM-EDX analyses of samples DR7-001 and DR7-002 using a Tescan Vega3 scanning electron microscope (SEM) at operating conditions of 30 kV and 15 nA for imaging; the Energy Dispersive Spectrometry (EDS) chemical characterization and element mapping was done using a JEOL 8900 operating at 15 kV and 40 nA for quantitative analyses of oxides; counting times were 30 s peak and 15 s background at USGS lab in Menlo Park in 2017.

95

### 3. Methodology

#### 3.1. Sample preparation

In order to exclude possible U-loss during the sample preparation when goethite grains are sonicated in a distilled water the leaching experiments were conducted. Millimetre-size fragments of goethite were manually extracted from the DR7-001 sample which represented dark-brown clast of the breccia and a yellow-brown vein material (Fig. 1B,C). At the first stage the massive single fragments in the closed Teflon vials with 3 ml of distilled deionized water (Barnsted) were sonicated for 15 min at room temperature without extra cooling. The solution was removed by the mechanical pipette for subsequent chemical

100



analyze. At the second stage the remained grains were dried at room temperature for 24 hours and crushed in the Teflon vial  
105 by the molybdenum stick ( $< 300 \mu\text{m}$ ) to increase their specific surface area. The crushed grains were sonicated in distilled  
deionized water (Barnsted; 3 ml) for extra 15 min at room temperature without extra cooling. After the solutions were left for  
24 hours for the sinking of the small floating particles. The uppermost 1 ml of the solution was carefully moved to a new  
beaker and nitric acid was added up to 5%  $\text{HNO}_3$  solutions (50–150  $\mu\text{l}$ ). Uranium and Th contents were measured by  
ELEMENT 2 ICP mass-spectrometer at the Institute of Precambrian Geology and Geochronology RAS. The full procedural  
110 blanks were obtained by the parallel procedures with an empty beaker. The total U and Th content of the sample was determined  
in the same way after its complete dissolution in the mixture of aqua regia (200  $\mu\text{l}$ ) with HF (250  $\mu\text{l}$ ) and  $\text{HClO}_4$  (10  $\mu\text{l}$ ) for 15  
h at  $110^\circ \text{C}$  in a closed Teflon vial in thermostat. Due to described analytical procedure the obtained U and Th contents in the  
leaching solutions are semi-quantitative.

### 3.2. (U-Th)/He dating

115 Eight millimeter-size fragments of goethite mineralization were manually extracted for (U-Th)/He dating from three different  
parts of the DR7-001 sample: two dark-brown clasts of the breccia and a yellow-brown vein from the completely altered rock  
(Fig. 1B,C; Table 2). Subsamples from the yellow-brown vein material and from dark-brown gains were treated as separate  
samples (1-8). Samples were derived from the inner part of the original sample and were not washed.

#### 3.2.1. Measurement of radiogenic $^4\text{He}$ contents

120 For each measurement,  $\sim 1\text{--}3$  mg fragments of goethite grains were placed in a quartz ampoule ( $\sim 1$  cm long) and sealed under  
a  $10^{-3}$  torr vacuum (Fig. 3). The sealing was done by the distilled water-based torch LIGA (Vasileostrovsky Electrochemical  
Plant). The sealed ampoule, via a special gateway, was placed in a high-temperature high-vacuum furnace of the magnetic  
sector MSU-G-01-M mass-spectrometer equipped with two SAES getter pumps (Spectron Analyt, IPGG RAS; Shukolyukov  
et al. 2012a,b). During heating, He easily diffuses through the thin quartz walls while U and other products of the sample  
125 decomposition remain in the ampoule. A Secondary Electron Multiplier (SEM) was used to determine the  $^4\text{He}^+$  beam intensity  
(cps). Calibration of the mass spectrometer was done using the RS-Pt reference material (Yakubovich et al. 2023). The standard  
uncertainty of the He measurement result was revealed from repeatability precision of 10 readings of  $^4\text{He}$ .

Goethite samples were step-heated at temperatures of  $350^\circ \text{C}$  for 30 min,  $550^\circ \text{C}$  for 10 min,  $900^\circ \text{C}$  for 10 min,  $1100^\circ \text{C}$  for  
15 min, and  $1150^\circ \text{C}$  until He stop to release (5 min in average). Samples 1 and 2 (ID 966, 969, Table 2) were step-heated  
130 under slightly different conditions, starting with a temperature of  $240^\circ \text{C}$ . This step-heating approach allows for monitoring  
the He release pattern from individual goethite grains as well as the excess hydrogen (ion  $\text{HD}^+$ ) in the camera of the mass-



spectrometer. Following the extraction of He, the ampoule was removed from the mass spectrometer for subsequent separation of U and Th.

The total procedural blank, determined by heating the empty quartz ampoules to 1100°C, corresponds to  $4.4 \pm 1.6 \times 10^{-10} \text{ cm}^3$

135 He at STP.

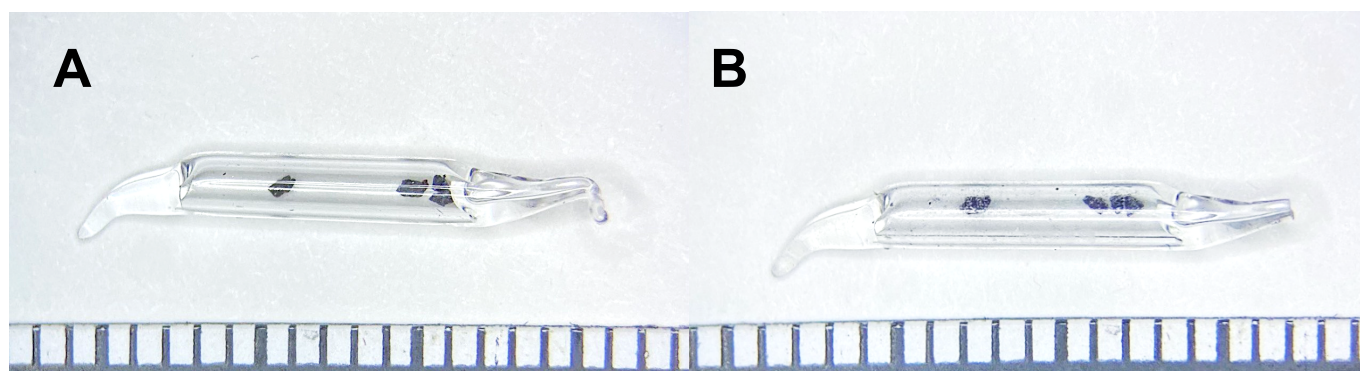


**Figure 3. Fragments of goethite in a sealed quartz ampoule (A) before heating; (B) after heating. Scale bar 1 mm.**

### 3.2.2. Measurement of U and Th Contents

140 The quartz ampoule with degassed samples was spiked with a  $^{230}\text{Th}$ - $^{235}\text{U}$  tracer and dissolved in a mixture of aqua regia (0.4 mL), concentrated hydrofluoric acid (0.5 mL), and perchloric acid (0.05 mL) in closed Teflon vials for 2 hours at 200° C on a hot plate followed by 15 h at 110° C in a thermostat. The solution was dried on a hot plate at 200° C. During this step, perchloric acid prevented the formation of low-soluble fluorine complexes, while most of Si evaporated in a form of  $\text{SiF}_4$ . The remaining precipitate was dissolved in 1.5 mL of 5% nitric acid and heated up to 80° C in an ultrasonic bath for 15 min prior the  
145 measurement of U and Th contents.  $^{235}\text{U}/^{238}\text{U}$  and  $^{230}\text{Th}/^{232}\text{Th}$  isotope ratios were measured on an ELEMENT XR ICP mass-spectrometer at the Vernadsky Institute of Geochemistry and Analytical Chemistry RAS. The total chemical procedure blank, determined by dissolution of the empty quartz ampoules (n=4) using the same settings, corresponds to  $1.30 \pm 1.26$  and  $5.8 \pm 4.4$   $10^{10}$  atoms of  $^{238}\text{U}$  and  $^{232}\text{Th}$  respectively.

The (U-Th)/He ages were calculated using IsoplotR software (Vermeesch, 2018). The combined analytical uncertainty was  
150 estimated based on the U, Th, and He measurement uncertainties and the uncertainty based on the blank determinations. The alpha-recoil corrections were not applied, because all analyzed samples are the fragments of large grains.

**Table 2. Results of (U-Th)/He Dating of Goethite Subsamples of DR7-001**



No.	ID	Type	Mass [mg]	U [ppm]	U [10 <sup>10</sup> at]	σ [%]	Th [ppm]	Th [10 <sup>10</sup> at]	σ [%]	Th/U	<sup>4</sup> He [cm <sup>3</sup> STP g <sup>-1</sup> ]	<sup>4</sup> He [10 <sup>10</sup> at]	σ [%]	age [Ma]	2σ
1	966		0.954	2.51	603	1.8	0.81	194	3.6	0.3	2.9 x 10 <sup>-6</sup>	7.54	2.3	9.1	0.5
2 <sup>a</sup>	969	Dark grains	7.197	1.86	3376	1.1	0.69	1258	2.1	0.4	3.4 x 10 <sup>-6</sup>	65.17	2.8	13.8	0.8
3	1015		1.946	2.62	1287	1.3	0.66	323	1.8	0.3	2.6 x 10 <sup>-6</sup>	13.73	3.7	7.9	0.6
4	1022		1.908	2.78	1338	1.8	0.81	387	2.0	0.3	3.1 x 10 <sup>-6</sup>	15.97	3.2	8.7	0.6
5 <sup>a</sup>	1031		2.973	2.43	1823	2.8	1.99	1491	2.4	0.8	4.3 x 10 <sup>-6</sup>	33.99	2.8	12.2	0.9
6	1032		3.115	2.25	1769	5.2	1.76	1379	5.0	0.8	2.6 x 10 <sup>-6</sup>	21.85	2.7	8.2	0.8
<b>Dark brown grains weighted mean<sup>c</sup> 8.6 ± 0.3</b>															
7	1033	Vein grains	1.782	1.36	613	2.2	3.30	1481	1.6	2.4	1.1 x 10 <sup>-6</sup>	5.40	8.7	4.4	0.8
8	1036		2.708	1.80	1232	2.5	4.90	3347	1.9	2.7	1.8 x 10 <sup>-6</sup>	12.70	3.9	4.9	0.4
<b>Yellowish brown vein weighted mean<sup>c</sup> 4.8 ± 0.4</b>															
	Empty Quartz ampoule <sup>b</sup>		28–56	--	1.3	97	--	6	74	--	--	1.1	37	--	--

155 The reported uncertainties of U, Th, and He measurements are the combined uncertainties calculated by summation in quadrature of measurement and blank uncertainties using a coverage factor of 1 which gives a level of confidence of approximately 65%.

<sup>a</sup>No. 2 and 5 ages not used in the calculation of mean age; see text in Results section for explanation.

<sup>b</sup>Contents of U, Th, and He in the quartz ampoule represent full analytical blank, which includes chemistry and steps of sample preparation (sealing, heating).

160 <sup>c</sup>The reported uncertainties of an age value is an expanded analytical uncertainty which include analytical uncertainty of U, Th, He measurements and factors addressed at the section 4.2. Error value corresponds to 95% level of confidence (2σ).

**Table 3. Results of the leaching experiments of Goethite Subsamples of DR7-001**

Sample	Stage	Weight, mg	U, ng	Th, ng	Th/U	Fraction of U-loss	Fraction of Th-loss
dark grain	first	5.628	0.03	0.01	0.26	0.3	0.3
	second		0.38	0.02	0.06	3.5	0.6
	residual		10.7	3.4	0.32	-	-
dark grain-2*	second	2.462	0.03	0.02	0.6	0.5	0.23
	residual		5.4	7.3	1.3	-	-
vein grain	first	6.212	0.01	0.02	1.4	0.12	0.10
	second		0.6	0.40	0.6	7.8	1.6
	total		8.4	24.7	2.5	-	-
vein grain-2*	second	1.890	0.11	0.19	1.7	3.0	1.7
	residual		3.6	10.9	3.0	-	-
blank	first	-	0.004	0.002	0.5	-	-
	second		0.01	0.005	0.7	-	-
	residual		0.01	0.02	1.8	-	-





165 Comment: \* grains were crushed and sonicated without previous step (first stage).

## 4. Results

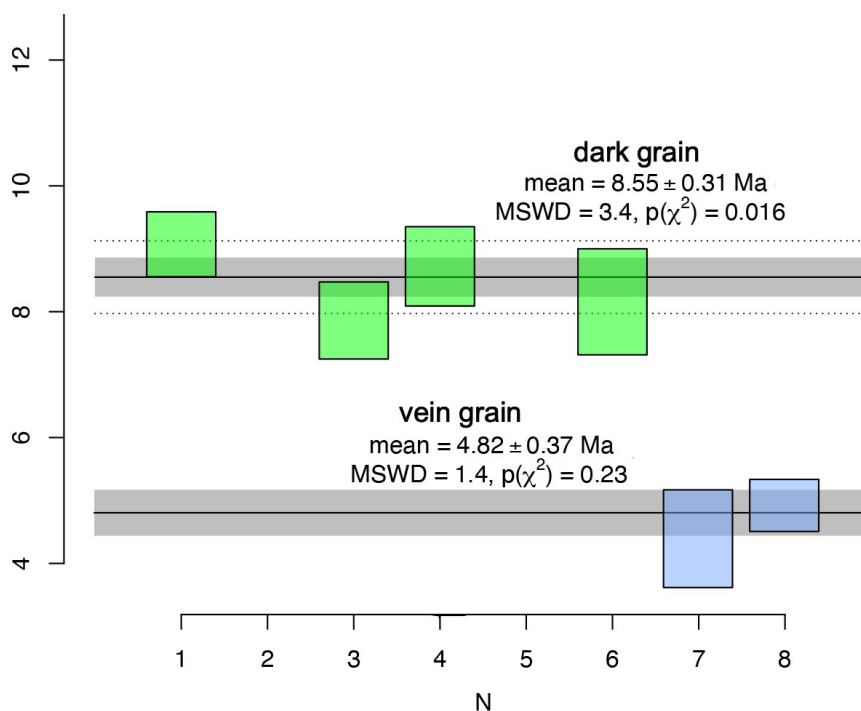
### 4.1. Leaching experiments

170 Chemical analyses of the distilled water leachates revealed the partial loss of U and Th from the subsamples (Table 3). The leaching of U and Th from the crushed subsample is more intensive than from a massive grain and reach up to 8% for U and less than 2% for Th. These findings are in an agreement with previous results of Fe- and Mn-oxides leaching experiments by a weak acids with acetate buffer (Konstantinova et al., 2018; Koschinsky and Hein, 2003) which implies U and Th adsorbed behavior. The leachates contain also some amount of Mn, Fe and Co, reflecting the presence of unstable/easily soluble mineral phases as well.

### 175 4.2. (U-Th)/He dating results

The (U-Th)/He ages for eight fragments of goethite from sample DR-7-001 included fragments of two sets of dark grains from two separate breccia goethite clasts (grains 1-4 and 5-6) and one set of yellow-brown vein samples (grains 7-8) (Table 2; Figure 4). The signals of He, U, and Th of all samples were markedly higher than the background level (empty quartz ampoule). The concentrations of U in the dark goethite grains range from 2.2–2.8 ppm, with Th/U ratios of 0.3–0.8. The concentration of U in the two vein subsamples is lower (1.36 and 1.8 ppm) and Th prevails over U (Th/U 2.4–2.7). Concentrations of  $^4\text{He}$  range from 2.6 to  $4.3 \times 10^{-6} \text{ cm}^3 \text{ STP g}^{-1}$  for the dark-brown grains and from 1.1 to  $1.8 \times 10^{-6} \text{ cm}^3 \text{ STP g}^{-1}$  for vein samples. Among the six dark goethite grains analyzed, one had an atypically low U concentration (1.86 ppm; Table 2), presumably due to improperly sealed quartz ampoule. Sample 5 (ID 1031) had an unusual high-temperature He release pattern ( $>1100^\circ$ , Fig. 6), which likely indicates the presence of He-retentive mineral inclusions.

185 The (U-Th)/He age of the remaining dark grains is consistent within the uncertainty of the measurements with a weighted mean value of  $8.6 \pm 0.3 \text{ Ma}$  ( $2\sigma$ ). The two yellow-brown vein samples had significantly younger reproducible ages, with a mean of  $4.8 \pm 0.4 \text{ Ma}$  ( $2\sigma$ ).



190 **Figure 4. Results of (U-Th)/He dating of goethite from DR7-001 subsamples. Error bars 2 $\sigma$ . Weighted mean plot constructed using IsoplotR software (Vermeesch, 2018).**

## 5. Discussion

### 5.1. Methodological implications

#### 5.1.1. Sample preparation

195 Due to the leaching experiments around 8% of U and 1.7% of Th can be remobilised from the sample by the fresh deionized distilled water, which is known to become chemically active after the contact with atmosphere (pH 5–6; Gurr, 1962). Goethite is not a water-soluble mineral therefore U release likely indicates its position beyond the crystal lattice or in some unstable phases. Th/U ratios of the grains (0.3 and 1.3 for dark grains; 2.5 and 3.0 for a vein material) are remarkably higher than those of leachates (0.06 and 0.6; 0.6 and 1.7, respectively; Table 3), which implies that U is easier to mobilize. This is in favor of  
 200 the adsorbed form of some of the U, rather than the presence of unstable phases with different Th/U ratios. The higher percent of U-loss from the crushed samples is also in agreement with this suggestion (Table 3).

The possible adsorbed behavior of U in goethite from the weathering environment was discussed by Shuster and Farley (2005) and Vasconcelos et al. (2013). The leaching experiments are also in agreement with the results of radiochemical experiments



that revealed that during the crystallization of hematite and goethite from ferrihydrite ( $\text{Fe}^{3+}$ ) $_2\text{O}_3 \cdot 0.5\text{H}_2\text{O}$ ), which is the least  
205 stable iron (oxyhydr)oxide, only part of uranium becomes leaching-resistant (Payne et al., 1994).

The proportion of U in adsorbed form relative to the U, which is incorporated into crystal lattice can differ from sample to  
sample. This is indirectly confirmed by the discussion in Vasconcelos et al. (2013), which suggest that various patterns of U-  
loss during the He release from the goethite samples possibly indicated different U position of the analyzed samples. Adsorbed  
behavior of some of the U does not affect strongly on applicability of the (U-Th)/He method due to the long alpha-stopping  
210 distances (Shuster et al., 2005). However, sonication of the samples in distilled water prior (U-Th)/He dating might result in  
U-loss and subsequent erroneous/over-dispersed ages for some of the samples.

### 5.1.2. Justification of the technique

(U-Th)/He ages of goethite subsamples are reproducible and have no signs of over-dispersion. This indicates that the proposed  
215 analytical approach is well suited for (U-Th)/He dating of goethite, and likely other Fe-(hydro)oxides. Encapsulating the  
individual goethite grains into the Qu ampoule exclude any U-loss during the sample degassing which is one of the major  
analytical concerns (Vasconcelos et al., 2013; Hofmann et al., 2020; Wu et al., 2019). The approach allows overheating of the  
sample with plenty of reserve. Based on our experience on He release from isoferroplatinum ( $\text{Pt}_3\text{Fe}$ ) Qu ampoule are robust to  
temperatures up to 1450°C (Shukolyukov et al., 2012b). One of the main disadvantages of the proposed technique is the  
220 relatively high blank of the Qu ampoule, which complicates analyse of very small and/or grains that are too young. The  
technique is quite sufficient for (U-Th)/He dating of mg-weighted samples of Neogene age as tested here, and require  
remarkably lower amount of the material than double- or multi aliquot approaches (Pidgeon et al., 2004; Wu et al., 2019). The  
technique also does not require keeping in a lab a dangerously explosive tank of pure  $\text{O}_2$  which have to be connected to the  
instrument for the  $\text{O}_2$  degassing procedure (Hofmann et al., 2020).

225 We suggest that application of the same technique on other mass-spectrometers might result in even better reproducibility of  
the (U-Th)/He ages of goethite samples. The secondary electron multiplier of the MSU-G-01-M mass-spectrometer has a  
reproducibility in a range of around 2.5%, application of these technique on the instruments equipped with a Faraday cup,  
which have better reproducibility (~1.2%; Yakubovich et al. 2023), might have produce even better values.

### 5.2 Geological implications

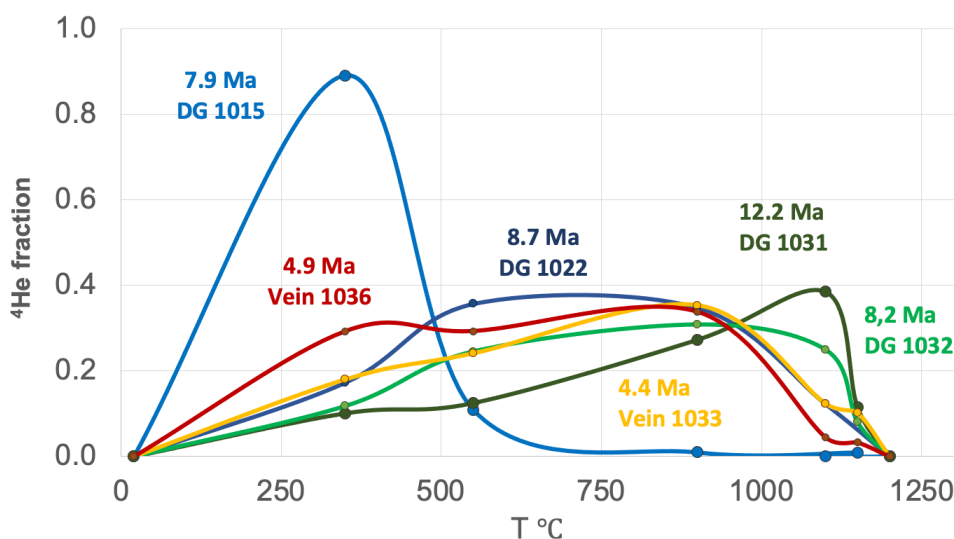
230 The results of the (U-Th)/He age dating of goethite grains from the slope of Chukchi Borderland produce a Neogene age  
formation. There are several factors that might potentially affect the mineral age results, such as He loss, radiation damage,  
recrystallisation, and fluid and mineral inclusions, which we discuss below.



### 5.2.1. Helium thermal retentivity

Goethite is predominantly He retentive under surface conditions (Cooperdock and Ault, 2020). The mineral is able to retain  
 235 around 80–95% of its radiogenic  $^4\text{He}$  for millions of years (Shuster et al. 2005; Deng et al. 2017; Hofmann et al., 2017). The  
 water temperature at 3400 m water depth within Chukchi Borderland slope is about  $-0.3\text{ }^\circ\text{C}$  (Zhang et al., 2021), therefore any  
 thermal loss of He seems unlikely, though it could be induced by local hydrothermal events.

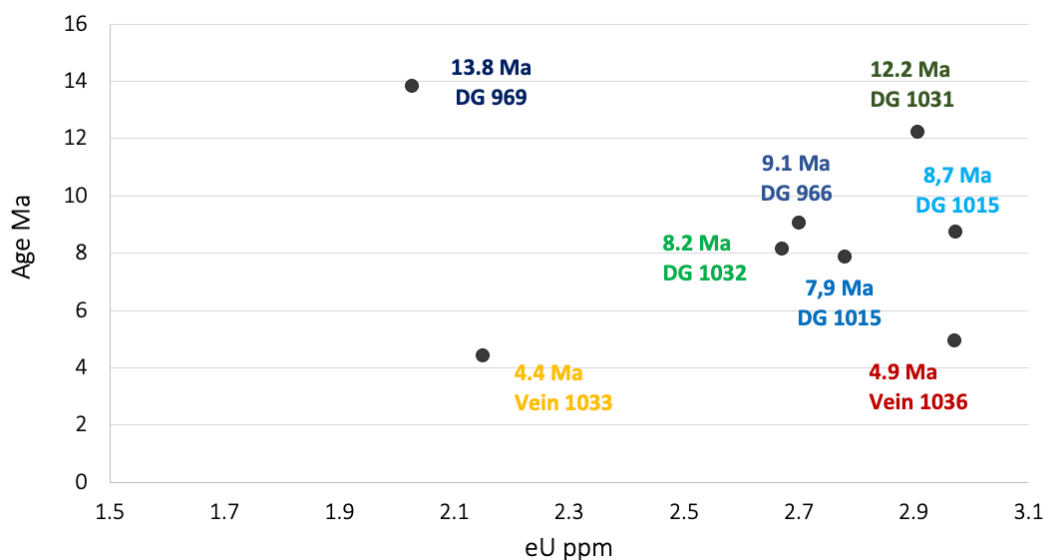
Heating the sample in a quartz ampoule does not allow simultaneous measurement of the He diffusion parameters, nevertheless  
 it does reflect the He retentivity of the sample. No correlation exists between the He release pattern and (U-Th)/He age,  
 240 reflecting an insignificant thermal loss of  $^4\text{He}$  (Fig. 5). Remarkable that He release pattern of the sample 3 (ID 1015)  
 significantly differs from the patterns of the other grains, despite its (U-Th)/He age is consistent with other measurements.



245 **Fig. 5. Helium release pattern from the goethite grains sealed in Quartz ampoule. All measurements were carried out under the same  
 time-temperature conditions. DG means fragments of the dark grain; vein – goethite from the yellowish vein material. Index is a  
 sample ID in the Table 2.**

### 5.2.2. Radiation damage

The He loss from goethite is strongly controlled by radiation damage, for example radiogenic defects and some other impurities  
 (e.g., Al) decrease the ability of He to diffuse (Bassal et al., 2022). There is no correlation of the age and modern eU content  
 250 of the samples (Fig. 6). The uniform (U-Th)/He ages of the petrological groups (clasts and vein) indicate limited impact of  
 the radiation damage on the dispersion of He ages.



255 **Figure 6. Goethite (U-Th)/He ages versus eU concentration of the samples. The effective modern uranium concentration (eU) was calculated based on the formulas given by (Flowers et al., 2023). DG means – fragments of the dark grain; vein – goethite from the yellowish vein material. Index is a sample ID in the Table 2.**

### 5.2.3. Mineral and fluid inclusions and impurities

The studied samples contain rare U- and Th-rich mineral inclusions, such as zircon and monazite, with sizes ranging between < 1 to 40  $\mu\text{m}$  (e.g. Fig. 2). If there was incomplete dissolution within the chemical procedure, the U-loss would result in an erroneously old and unreproducible ages, which might be the case of sample 5 (ID 1031).

260 Helium concentration of minerals fluid inclusions that formed during magmatic and hydrothermal processes typically does not exceed  $10^{-8} \text{ cm}^3 \text{ STP g}^{-1}$  (Stuart et al., 1994; Graupner et al., 2006), that is less than 1% of the total He of the studied samples and insignificant for our (U-Th)/He dating procedure.

Incorporation of Sm can be an additional source of  $^4\text{He}$  in goethite. Sm contents of the DR7-001 samples vary from 5.5 to 6 ppm (ICP-MS data; lithium-metaborate fused disks;  $n=3$ ), which implies that Sm would produce less than 0.25% of the He  
265 sample budget.

### 5.2.4. Recrystallization

Goethite is not stable in the near-surface environment and can undergo dissolution–recrystallization processes that reset its (U-Th)/He age (Monteiro et al., 2014). These processes enrich samples with low-soluble components that increase the Th/U ratios. This might be initiated by the presence of  $\text{Fe}^{2+}$  ions in the aquatic systems (Handler et al., 2014). Given that the vein has higher



270 Th/U ratios (2.5–2.7 vs 0.3–0.8 of the dark grains) and younger (U-Th)/He age ( $4.8 \pm 0.9$  Ma vs  $8.6 \pm 1.2$  Ma; Table 2), its newly  
formation due to the recrystallization of goethite cannot be ruled out.

### 5.2.5. Interpretation of (U-Th)/He ages

In additional to assessment of the all factors that might impact the (U-Th)/He ages, we include 10% ( $2\sigma$ ) uncertainty to the  
primary analytical uncertainty of the measurements based on the suggestion of (Monteiro et al., 2014). Thus, the dense dark-  
275 brown goethite have the age of  $8.6 \pm 1.2$  Ma ( $2\sigma$ ), and the vein material is younger,  $4.8 \pm 0.9$  Ma ( $2\sigma$ ). These values do not  
overlap within the extended uncertainty.

The (U-Th)/He ages reflect the time of mineral formation, recrystallization, or cooling below the closure temperature. Closure  
temperature of goethite varies over a wide range, from  $\sim 20$  to  $150^\circ$  C, depending on the diffusion domain sizes and distribution  
of the defects in the crystal lattice (Bassal et al., 2022). Thus, the uniform (U-Th)/He ages of the dark-brown grains  
280 accompanied by remarkably different He release patterns (Fig. 5) might be explained by cooling, only with the assumption of  
fast (1–2 Ma) host rocks uplift from  $\sim 2$ –4 km depth that took place  $\sim 9$  Ma ago. However, that assumption is inconsistent with  
the tectonic evolution of the Arctic region (e.g., Chian et al., 2016; Craddock and Houseknecht, 2016). Therefore, (U-Th)/He  
ages reflect a Neogene mineralization event in the Chukchi Borderland, Arctic Ocean.

## 6. Conclusion

285 Reproducible non-over-dispersed (U-Th)/He ages is achieved using our proposed analytical approach, which involves sealing  
the sample in quartz ampoule for He release is well suited for (U-Th)/He dating of Fe-hydroxides; this techniques allows for  
the determination of U, Th, and He on the same subsample aliquot. Our data also indicate that significant fraction of U can be  
leached from goethite samples during sonication in the distilled water, implying that this step of goethite sample preparation  
for (U-Th)/He dating should be taken with caution.

290

(U-Th)/He ages of goethite from the slope of the Chukchi Borderland formed during a Neogene mineralization event ( $8.6 \pm 1.2$   
Ma). The younger age of the yellow-brown vein material ( $4.8 \pm 0.9$  Ma) can be explained by an episode of later-stage  
mineralization and/or recrystallization. Alternatively, the small number of dated samples and distribution of samples may  
preclude being able to detect continuous Neogene mineralization from 8.6 Ma to 4.8 Ma throughout the region. Further  
295 investigations and a larger sample set are recommended for a comprehensive understanding of the geological evolution of the  
region.



## Competing interests

The contact author has declared that none of the authors has any competing interest.

## Acknowledgements

300 We thank James R. Hein and Kira Mizell from U.S. Geological Survey for the provision of samples used in this study and for reviews.

This research was supported by RSF 22-77-10088. Chemical analyses done by M.O. Anosova were funded by the State Assignment of the Vernadsky Institute of Geochemistry and Analytical Chemistry, Russian Academy of Sciences.

## References

- 305 Ansart, C., Quantin, C., Calmels, D., Allard, T., Roig, J. Y., Coueffe, R., Heller, B., Pinna-Jamme, R., Nouet, J., Reguer, S., Vantelon, D., and Gautheron, C.: (U-Th)/He Geochronology Constraints on Lateritic Duricrust Formation on the Guiana Shield, *Front. Earth Sci.*, 10, 1–19, <https://doi.org/10.3389/feart.2022.888993>, 2022.
- Bassal, F., Heller, B., Roques, J., Balout, H., Tassan-Got, L., Allard, T., and Gautheron, C.: Revealing the radiation damage and Al-content impacts on He diffusion in goethite, *Chem. Geol.*, 611, <https://doi.org/10.1016/j.chemgeo.2022.121118>, 2022.
- 310 Basu, S., Stuart, F. M., Klemm, V., Korschinek, G., Knie, K., and Hein, J. R.: Helium isotopes in ferromanganese crusts from the central Pacific Ocean, *Geochim. Cosmochim. Acta*, 70, 3996–4006, <https://doi.org/10.1016/j.gca.2006.05.015>, 2006.
- Benites, M., Hein, J. R., Mizell, K., Farley, K. A., Treffkorn, J., and Jovane, L.: Geochemical insights into formation of enigmatic ironstones from Rio Grande rise, South Atlantic Ocean, *Mar. Geol.*, 444, 106716, <https://doi.org/10.1016/j.margeo.2021.106716>, 2022.
- 315 Brumley, K., Miller, E. L., Konstantinou, A., Grove, M., Meisling, K. E., and Mayer, L. A.: First bedrock samples dredged from submarine outcrops in the Chukchi Borderland, Arctic Ocean, *Geosphere*, 11, 76–92, <https://doi.org/10.1130/GES01044.1>, 2015.
- Chian, D., Jackson, H. R., Hutchinson, D. R., Shimeld, J. W., Oakey, G. N., Lebedeva-Ivanova, N., Li, Q., Saltus, R. W., and Mosher, D. C.: Distribution of crustal types in Canada Basin, Arctic Ocean, *Tectonophysics*, 691, 8–30, <https://doi.org/10.1016/j.tecto.2016.01.038>, 2016.
- 320 Cooperdock, E. H. G. and Ault, A. K.: Iron oxide (U-Th)/he thermochronology: New perspectives on faults, fluids, and heat, *Elements*, 16, 319–324, <https://doi.org/10.2138/gselements.16.5.319>, 2020.
- Craddock, W. H. and Houseknecht, D. W.: Cretaceous-Cenozoic burial and exhumation history of the Chukchi shelf, offshore Arctic Alaska, *Am. Assoc. Pet. Geol. Bull.*, 100, 63–100, <https://doi.org/10.1306/09291515010>, 2016.



- 325 Deng, X. D., Li, J. W., and Shuster, D. L.: Late Mio-Pliocene chemical weathering of the Yulong porphyry Cu deposit in the eastern Tibetan Plateau constrained by goethite (U–Th)/He dating: Implication for Asian summer monsoon, *Earth Planet. Sci. Lett.*, 472, 289–298, <https://doi.org/10.1016/j.epsl.2017.04.043>, 2017.
- Farley, K. a. and Stockli, D. F.: (U–Th)/He Dating of Phosphates: Apatite, Monazite, and Xenotime, *Rev. Mineral. Geochemistry*, 48, 559–577, <https://doi.org/10.2138/rmg.2002.48.15>, 2002.
- 330 Flowers, R. M., Zeitler, P. K., Danišik, M., Reiners, P. W., Gautheron, C., Ketcham, R. A., Metcalf, J. R., Stockli, D. F., Enkelmann, E., and Brown, R. W.: (U–Th)/He chronology: Part 1. Data, uncertainty, and reporting, *Bull. Geol. Soc. Am.*, 135, 104–136, <https://doi.org/10.1130/B36266.1>, 2023.
- Graupner, T., Niedermann, S., Kempe, U., Klemd, R., and Bechtel, A.: Origin of ore fluids in the Muruntau gold system: Constraints from noble gas, carbon isotope and halogen data, *Geochim. Cosmochim. Acta*, 70, 5356–5370, 335 <https://doi.org/10.1016/j.gca.2006.08.013>, 2006.
- Gurr, E.: Effect of heat on the pH of water and aqueous dye solutions, *Nature*, 4847, 1199–1200, 1962.
- Handler, R. M., Friedrich, A. J., Johnson, C. M., Rosso, K. M., Beard, B. L., Wang, C., Latta, D. E., Neumann, A., Pasakarnis, T., Premaratne, W. A. P. J., and Scherer, M. M.: Fe(II)-catalyzed recrystallization of goethite revisited, *Environ. Sci. Technol.*, 48, 11302–11311, <https://doi.org/10.1021/es503084u>, 2014.
- 340 Hein, J. R., Konstantinova, N., Mikesell, M., Mizell, K., Fitzsimmons, J. N., Lam, P. J., Jensen, L. T., Xiang, Y., Gartman, A., Cherkashov, G., Hutchinson, D. R., and Till, C. P.: Arctic Deep Water Ferromanganese-Oxide Deposits Reflect the Unique Characteristics of the Arctic Ocean, *Geochemistry, Geophys. Geosystems*, 18, 3771–3800, <https://doi.org/10.1002/2017GC007186>, 2017.
- Heller, B. M., Riffel, S. B., Allard, T., Morin, G., Roig, J. Y., Couëffé, R., Aertgeerts, G., Derycke, A., Ansart, C., Pinna- 345 Jamme, R., and Gautheron, C.: Reading the climate signals hidden in bauxite, *Geochim. Cosmochim. Acta*, 323, 40–73, <https://doi.org/10.1016/j.gca.2022.02.017>, 2022.
- Hofmann, F., Reichenbacher, B., and Farley, K. A.: Evidence for >5 Ma paleo-exposure of an Eocene–Miocene paleosol of the Bohnerz Formation, Switzerland, *Earth Planet. Sci. Lett.*, 465, 168–175, <https://doi.org/10.1016/j.epsl.2017.02.042>, 2017.
- Hofmann, F., Treffkorn, J., and Farley, K. A.: U-loss associated with laser-heating of hematite and goethite in vacuum during 350 (U–Th)/He dating and prevention using high O<sub>2</sub> partial pressure, *Chem. Geol.*, 532, 119350, <https://doi.org/10.1016/j.chemgeo.2019.119350>, 2020.
- Konstantinova, N., Cherkashov, G., Hein, J. R., Mirão, J., Dias, L., Madureira, P., Kuznetsov, V., and Maksimov, F.: Composition and characteristics of the ferromanganese crusts from the western Arctic Ocean, *Ore Geol. Rev.*, 87, 88–99, <https://doi.org/10.1016/j.oregeorev.2016.09.011>, 2017.
- 355 Konstantinova, N., Hein, J. R., Gartman, A., Mizell, K., Barrulas, P., Cherkashov, G., Mikhailik, P., and Khanchuk, A.: Mineral phase-element associations based on sequential leaching of ferromanganese crusts, Amerasia Basin Arctic ocean, *Minerals*, 8,





- <https://doi.org/10.3390/min8100460>, 2018.
- Koschinsky, A. and Hein, J. R.: Uptake of elements from seawater by ferromanganese crusts: Solid-phase associations and seawater speciation, *Mar. Geol.*, 198, 331–351, [https://doi.org/10.1016/S0025-3227\(03\)00122-1](https://doi.org/10.1016/S0025-3227(03)00122-1), 2003.
- 360 Monteiro, H. S., Vasconcelos, P. M., Farley, K. A., Spier, C. A., and Mello, C. L.: (U-Th)/He geochronology of goethite and the origin and evolution of cangas, *Geochim. Cosmochim. Acta*, 131, 267–289, <https://doi.org/10.1016/j.gca.2014.01.036>, 2014.
- Payne, T. E., Davis, J. A., and Waite, T. D.: Uranium Retention by Weathered Schists - The Role of Iron Minerals, *Radiochim. Acta*, 66–67, 297–304, <https://doi.org/10.1524/ract.1994.6667.special-issue.297>, 1994.
- 365 Pidgeon, R. T., Brander, T., and Lippolt, H. J.: Late Miocene (U+Th)-4He ages of ferruginous nodules from lateritic duricrust, Darling Range, Western Australia, *Aust. J. Earth Sci.*, 51, 901–909, <https://doi.org/10.1111/j.1400-0952.2004.01094.x>, 2004.
- Reiners, P. W., Chan, M. A., and Evenson, N. S.: (U-Th)/He geochronology and chemical compositions of diagenetic cement, concretions, and fracture-filling oxide minerals in mesozoic sandstones of the Colorado Plateau, *Bull. Geol. Soc. Am.*, 126, 1363–1383, <https://doi.org/10.1130/B30983.1>, 2014.
- 370 Riffel, S. B., Vasconcelos, P. M., Carmo, I. O., and Farley, K. A.: Goethite (U–Th)/He geochronology and precipitation mechanisms during weathering of basalts, *Chem. Geol.*, 446, 18–32, <https://doi.org/10.1016/j.chemgeo.2016.03.033>, 2016.
- Shukolyukov, Y. A., Yakubovich, O. V., Yakovleva, S. Z., Sal’nikova, E. B., Kotov, A. B., and Rytsk, E. Y.: Geothermochronology based on noble gases: III. Migration of radiogenic He in the crystal structure of native metals with applications to their isotopic dating, *Petrology*, 20, 1–20, <https://doi.org/10.1134/S0869591112010043>, 2012a.
- 375 Shukolyukov, Y. A., Yakubovich, O. V., Mochalov, A. G., Kotov, A. B., Sal’nikova, E. B., Yakovleva, S. Z., Korneev, S. I., and Gorokhovskii, B. M.: New geochronometer for the direct isotopic dating of native platinum minerals (190Pt-4He method), *Petrology*, 20, 491–505, <https://doi.org/10.1134/S0869591112060033>, 2012b.
- Shukolyukov, Y. A., Yakubovich, O. V., Mochalov, A. G., Kotov, A. B., Sal’nikova, E. B., Yakovleva, S. Z., Korneev, S. I., and Gorokhovskii, B. M.: New geochronometer for the direct isotopic dating of native platinum minerals (190Pt-4He method), *Petrology*, 20, 491–505, <https://doi.org/10.1134/S0869591112060033>, 2012c.
- 380 Shuster, D. L. and Farley, K. A.: Diffusion kinetics of proton-induced He in quartz, *Geochim. Cosmochim. Acta*, 69, 2349–2359, <https://doi.org/10.1016/j.gca.2004.11.002>, 2005.
- Shuster, D. L., Vasconcelos, P. M., Heim, J. A., and Farley, K. A.: Weathering geochronology by (U-Th)/He dating of goethite, *Geochim. Cosmochim. Acta*, 69, 659–673, <https://doi.org/10.1016/j.gca.2004.07.028>, 2005.
- 385 Strutt, R.: Helium and Radio-activity in Rare and Common Minerals, *Proc. R. Soc. London. Ser. A, Contain. Pap. a Math. Phys. Character*, 80, 572–594, 1908.
- Strutt, R.: The Accumulation of Helium in Geological Time, *Proc. R. Soc. London. Ser. A, Contain. Pap. a Math. Phys. Character*, 83, 298–301, 1909.



- Stuart, F. M., Turner, G., Duckworth, R. C., and Fallick, A. E.: Helium isotopes as tracers of trapped hydrothermal fluids in  
390 ocean- floor sulfides, *Geology*, 22, 823–826, [https://doi.org/10.1130/0091-7613\(1994\)022<0823:HIATOT>2.3.CO;2](https://doi.org/10.1130/0091-7613(1994)022<0823:HIATOT>2.3.CO;2), 1994.
- Vasconcelos, P. M., Heim, J. A., Farley, K. A., Monteiro, H., and Waltenberg, K.:  $^{40}\text{Ar}/^{39}\text{Ar}$  and  $(\text{U-Th})/\text{He} - 4\text{He}/3\text{He}$   
geochronology of landscape evolution and channel iron deposit genesis at Lynn Peak, Western Australia, *Geochim.*  
*Cosmochim. Acta*, 117, 283–312, <https://doi.org/10.1016/j.gca.2013.03.037>, 2013.
- Verhaert, M., Gautheron, C., Dekoninck, A., Vennemann, T., Pinna-Jamme, R., Mouttaqi, A., and Yans, J.: Unravelling the  
395 Temporal and Chemical Evolution of a Mineralizing Fluid in Karst-Hosted Deposits: A Record from Goethite in the High  
Atlas Foreland (Morocco), *Minerals*, 12, <https://doi.org/10.3390/min12091151>, 2022.
- Vermeesch, P.: IsoplotR: A free and open toolbox for geochronology, *Geosci. Front.*, 9, 1479–1493,  
<https://doi.org/10.1016/j.gsf.2018.04.001>, 2018.
- Wernicke, R. S. and Lippolt, H. J.: Botryoidal hematite from the Schwarzwald ( Germany )" heterogeneous uranium  
400 distributions and their bearing on the helium dating method, 114, 287–300, 1993.
- Wu, L. Y., Stuart, F. M., Di Nicola, L., Heizler, M., Benvenuti, M., and Hu, R. Z.: Multi-aliquot method for determining  
 $(\text{U} + \text{Th})/\text{He}$  ages of hydrothermal hematite: Returning to Elba, *Chem. Geol.*, 504, 151–157,  
<https://doi.org/10.1016/j.chemgeo.2018.11.005>, 2019.
- Yakubovich, O., Podolskaya, M., Vikentyev, I., Fokina, E., and Kotov, A.: U-Th-He Geochronology of Pyrite from the Uzelga  
405 VMS Deposit ( South Urals )— New Perspectives for Direct Dating of the Ore-Forming Processes, *Minerals*, 10, 1–20,  
<https://doi.org/10.3390/min10070629>, 2020.
- Yakubovich, O. V., Shukolyukov, Y. a., Kotov, a. B., Brauns, M., Samsonov, a. V., Komarov, a. N., Yakovleva, S. Z.,  
Sal'nikova, E. B., and Gorokhovskii, B. M.: U-Th-He dating of native gold: First results, problems, and outlooks, *Petrology*,  
22, 429–437, <https://doi.org/10.1134/S0869591114050075>, 2014.
- 410 Yakubovich, O. V., Stuart, F. M., Ivanova, E. S., and Gervilla, F.: Constant  $4\text{He}$  Concentration and  $^{190}\text{Pt}$ - $4\text{He}$  age of Detrital  
Pt-Alloy Grains from the Santiago River, Ecuador: Potential as a  $4\text{He}$  Mineral Reference Material, *Geostand. Geoanalytical*  
*Res.*, 47, 957–968, <https://doi.org/10.1111/ggr.12502>, 2023.
- Yakubovich, O. V., Gedz, A. M., Vikentyev, I. V., Kotov, A. B., and Gorokhovskii, B. M.: Migration of Radiogenic Helium in  
the Crystal Structure of Sulfides and Prospects of Their Isotopic Dating, *Petrology*, 27, 59–78,  
415 <https://doi.org/10.1134/S0869591118050089>, 2019.